J|A|C|S
ARTICLES
Published on Web 10/23/2004

Redox Inactivation of Human 15-Lipoxygenase by Marine-Derived Meroditerpenes and Synthetic Chromanes: Archetypes for a Unique Class of Selective and Recyclable Inhibitors

Robert H. Cichewicz,[†,‡] Victor A. Kenyon,[†] Stephanie Whitman,[†] Nancy M. Morales,[†,‡] Joanne F. Arguello,[†,‡] Theodore R. Holman,*[,†] and Phillip Crews*[,†,‡]

Contribution from the Department of Chemistry and Biochemistry and Institute for Marine Sciences, University of California, Santa Cruz, California 95064

Received July 1, 2004; E-mail: holman@chemistry.ucsc.edu; phil@chemistry.ucsc.edu

Abstract: The selective inhibition of human 15-lipoxygenase (15-hLO) could serve as a promising therapeutic target for the prevention of atherosclerosis. A screening of marine sponges revealed that crude extracts of *Psammocinia* sp. exhibited potent 15-hLO inhibitory activity. Bioassay-guided fractionation led to the isolation of chromarols A−E (**8**−**12**) as potent and selective inhibitors of 15-hLO. An additional 22 structurally related compounds, including meroditerpenes from the same *Psammocinia* sp. (**3**, **4**, **13**−**16**) and our pure compound repository (**17**, **18**), commercially available tocopherols (**19**−**24**), and synthetic chromanes (**25**−**32**), were evaluated for their ability to inhibit human lipoxygenases. The 6-hydroxychromane moiety found in chromarols A−D was identified as essential for the selective redox inhibition of 15-hLO. Furthermore, the oxidized form of the 6-hydroxychromane could be reduced by ascorbate, suggesting a potential regeneration pathway for these inhibitors in the body. This pharmacophore represents a promising paradigm for the development of a unique class of recyclable 15-hLO redox inhibitors for the treatment of atherosclerosis.

Introduction

Human lipoxygenases (hLO) are non-heme iron-containing catalysts that guide the stereospecific incorporation of molecular oxygen into long-chain fatty acid substrates.[1,2] The products of hLO catalysis have been implicated as important intercellular signal mediators in a variety of diseases including atherosclerosis (human 15-lipoxygenase), cancer (human 12-lipoxygenase), inflammation (human 8-lipoxygenase), and asthma (human 5-lipoxygenase).[3] Therefore, the selective inhibition of specific hLO isoforms is a promising therapeutic modality for the treatment of these disorders.

Our laboratories continue to be involved in a collaborative effort to identify potent ($IC_{50} \leq 1\ \mu M$) and selective (≥100-fold IC_{50} differential) fold inhibitors of specific hLO isoforms. Previously, we disclosed that marine sponges could serve as an important resource for the discovery of novel hLO inhibitors.[4] From these studies, several relevant sponge-derived terpenoids and complex organobromines were identified. Selected pertinent examples from these discoveries are illustrated in Figure 1, and their activities are summarized below. For example, puupehenone (**1**) and 21-chloropuupehenone (**2**) from *Hyrtios* sp. were reported as potent but nonselective inhibitors of both human platelet 12-lipoxygenase (12-hLO) ($IC_{50} = 8.3 \pm 1.7$ and $0.71 \pm 0.05\ \mu M$, respectively) and human reticulocyte 15-lipoxygenase (15-hLO) ($IC_{50} = 0.76 \pm 0.07$ and $0.83 \pm 0.04\ \mu M$, respectively). Likewise, jaspic acid (**3**) and jaspaquinol (**4**) from *Suberea* sp. were also shown to inhibit both 12-hLO ($IC_{50} = 0.7 \pm 0.05$ and $4.5 \pm 1.0\ \mu M$, respectively) and 15-hLO ($IC_{50} = 1.4 \pm 0.2$ and $0.3 \pm 0.1\ \mu M$, respectively) in a relatively equipotent fashion. In contrast, the sponge-derived terpenoid, igerellin (**5**), displayed weak but selective activity against 15-hLO ($IC_{50} = 17 \pm 10\ \mu M$) versus 12-hLO ($IC_{50} > 200\ \mu M$).[5] More recently, we have observed that certain sponge-derived polybrominated phenol ethers such as 3,4,5,6,2′,4′-hexabromodiphenol ether (**6**) (12-hLO $IC_{50} = 0.7 \pm 0.2\ \mu M$; 15-hLO $IC_{50} = 1.8 \pm 0.4\ \mu M$) and polymeric tyrosine derivatives such as bastadine 2 (**7**) (12-hLO $IC_{50} = 0.4 \pm 0.1\ \mu M$; 15-hLO $IC_{50} = 2.0 \pm 0.4\ \mu M$) are also potent but nonselective inhibitors of 12-hLO and 15-hLO.[6] Unfortunately, none of these marine-derived compounds exhibited sufficient selectivity and/or

[†] Department of Chemistry and Biochemistry.
[‡] Institute for Marine Sciences.

(1) Kühn, H.; Walther, M.; Kuban, R. J. *Prostaglandins Lipid Mediat.* **2002**, *68*−*69*, 263−290.
(2) Steele, V. E.; Holmes, C. A.; Hawk, E. T.; Kopelovich, L.; Lubet, R. A.; Crowell, J. A.; Sigman, C. C.; Kelloff, G. J. *Exp. Opin. Invest. Drugs* **2000**, *9*, 2121−2138.
(3) Dailey, L. A.; Imming, P. *Curr. Med. Chem.* **1999**, *6*, 389−398.
(4) Carroll, J.; Jonsson, E. N.; Ebel, R.; Hartman, M. S.; Holman, T. R.; Crews, P. *J. Org. Chem.* **2001**, *66*, 6847−6851.
(5) Amagata, T.; Whitman, S.; Johnson, T. A.; Stessman, C. C.; Loo, C. P.; Lobkovsky, E.; Clardy, J.; Crews, P.; Holman, T. R. *J. Nat. Prod.* **2003**, *66*, 230−235.
(6) Segraves, E. N.; Shah, R. R.; Segraves, N. L.; Johnson, T. A.; Whitman, S.; Sui, J. K.; Kenyon, V.; Cichewicz, R. H.; Crews, P.; Holman, T. R. *J. Med. Chem.* **2004**, *47*, 4060−4065.

10.1021/ja046082z CCC: $27.50

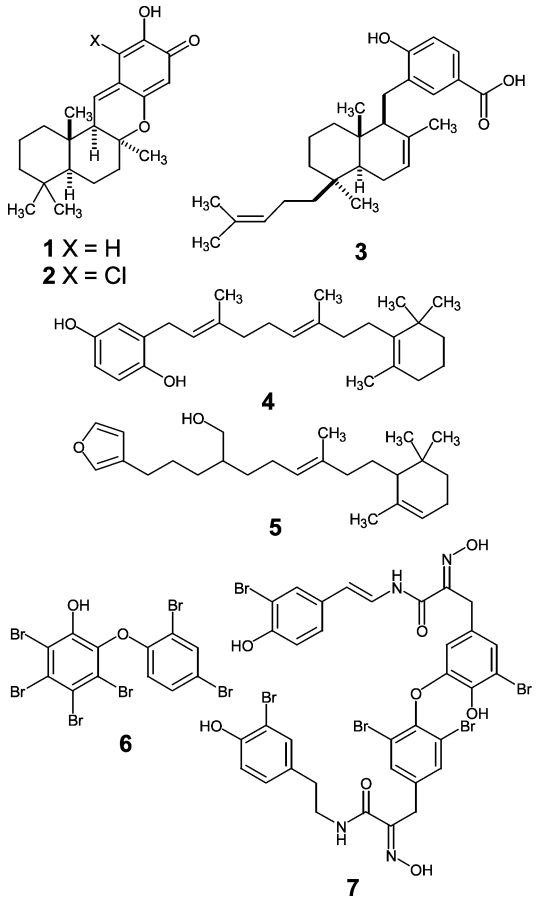

Figure 1. Structures of marine sponge-derived lipoxygenase inhibitors of diverse biosynthetic origins.

potency against either 12-hLO or 15-hLO isoforms to warrant pharmacological interest. Inspired by the need for isozyme-specific modulators of hLO, we have renewed our efforts to discover novel, potent, and selective hLO inhibitors.

As part of this endeavor, we have focused on the discovery of inhibitors of 15-hLO that exhibit improved potency and selectivity. Interest in inhibitors of this enzyme stems from the growing body of evidence that implicates 15-hLO in pro-atherogenic processes. It has been demonstrated that increased levels of 15-hLO are present in atherosclerotic plaques.[7] Furthermore, the products of 15-hLO can function as pro-atherogenic signal mediators.[1,8] While many facets of this process remain unclear, more than ample evidence currently exists for a pathogenic role of 15-hLO in atherosclerosis.[9]

The goal of the present study was to identify additional promising marine-derived sponge leads and determine their active constituents. As part of this strategy, a *Psammocinia* collection from the Madang region of Papua New Guinea (UCSC collection number 01236) was observed to exhibit potent activity against 15-hLO. *Psammocinia* spp. (Dictyoceratida, Irciniidae) are proving to be a rich source of bioactive and chemically diverse marine natural products. We recently reported the isolation of the novel cancer cell cytotoxin, psymberin[10] (irciniastatin A[11]), from a pooled collection of a different Papua New Guinean *Psammocinia* sp. Additional discoveries from *Psammocinia* include the hexapeptide cyclocinamide A, polyketides, furanosesterpenes, and polybrominated phenol ethers.[10]

In this report, the active hLO inhibitory constituents from *Psammocinia* are presented. On the basis of these discoveries, additional relevant project goals were identified. This included comparing the activities of the new *Psammocinia*-derived metabolites against a variety of structurally related compounds from three sources: (1) the UCSC marine natural products repository, (2) commercial sources, and (3) synthetic derivatives prepared for this investigation. Further studies were initiated in order to define the mode of action of these new inhibitors. This investigation has provided evidence for the basic structural requirements of a unique series of selective, redox-recyclable 15-hLO inhibitors that may prove beneficial in the management of atherosclerosis.

Results and Discussion

Summary of Compounds Studied. Bioassay-guided fractionation of the active *Psammocinia* extract led to the isolation of a series of hLO inhibitory meroditerpenes. These compounds can be classified into three discrete sets, groups A−C, on the basis of their biological activity and structural features. Group A metabolites (Figure 2) consist of a series of new meroditerpene chromanes and have been named chromarols A−E (**8**−**12**). Group B compounds **4** and **13**−**16** represent a collection of acyclic and monocyclic meroditerpenes (Figure 3). These five previously described metabolites are jaspaquinol (**4**), cacospongin B (**13**), cacospongin D (**14**), 1,4-dihydroxy-2-tetraprenylbenzene (**15**), and 4-hydroxy-3-tetraprenylbenzoic acid (**16**). All of these compounds are reported from *Psammocinia* for the first time. Group C is composed of three (**3**, **17**, **18**) marine-derived polycyclic meroditerpenes (Figure 4). Compound **3**, jaspic acid, is reported here from *Psammocinia* for the first time. The sponge-derived compounds **17** and **18**, strongylophorins-2 and -3, respectively, were originally isolated from a *Strongylophora* sp. and were obtained from the UCSC pure compound repository. This investigation was further expanded to include two additional sets of structurally related compounds. Group D is comprised of six tocopherols, compounds **19**−**24**, obtained from commercial sources (Figure 5). Finally, group E constitutes a set of eight synthetic chromanes, compounds **25**−**32**, possessing varying degrees of methylation and hydroxylation (Figure 6).

Structure Elucidation of Chromarols A−E (8−12). Chromarol A (**8**) possessed a molecular formula of $C_{26}H_{36}O_2$ with nine degrees of unsaturation based on HRESIMS analysis (*m*/*z* 381.2796 $[M + H]^+$, calcd 381.2794). This was consistent with NMR data (^{1}H, ^{13}C, and DEPT; see Tables 1 and 2) that showed the presence of five methyl, seven methylene, six methine, and eight quaternary carbons accounting for $C_{26}H_{35}$. ^{13}C NMR shift data revealed one aliphatic (δ_C 76.3 s) and two aromatic (δ_C 149.6 and 148.6 s) residues attached to heteroatoms. The presence of one exchangeable proton (δ_H 3.85) combined with the molecular formula constraint of two oxygen atoms supported the existence of hydroxyl and ether moieties in **8**.

(7) Ylä-Herttuala, S.; Rosenfeld, M. E.; Parthasarath, S.; Glass, C. K.; Sigal, E.; Witztum, J. T.; Steinberg, D. *Proc. Natl. Acad. Sci. U.S.A.* **1990**, *87*, 6959−6963.
(8) Schewe, T. *Biol. Chem*. **2002**, *383*, 365−374.
(9) Cornicelli, J. A.; Trivedi, B. K. *Curr. Pharm. Des.* **1999**, *5*, 11−20.
(10) Cichewicz, R. H.; Valeriote, F. A.; Crews, P. *Org. Lett*. **2004**, *6*, 1951−1954 and references therein.
(11) Pettit, G. R.; Xu, J.-P.; Chapuis, J.-C.; Pettit, R. K.; Tackett, L. P.; Doubek, D. L.; Hooper, J. N. A.; Schmidt, J. M. *J. Med. Chem.* **2004**, *47*, 1149−1152.

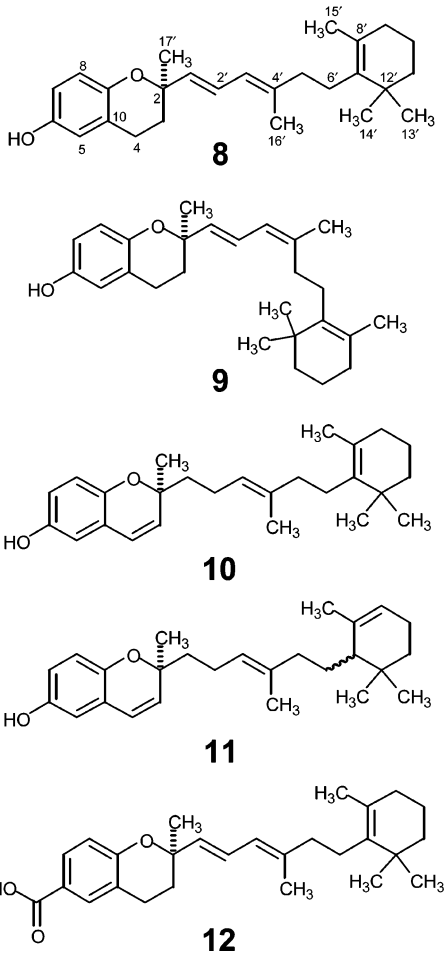

Figure 2. Group A: new marine-derived chromarols A−E (**8**−**12**) from *Psammocinia* sp.

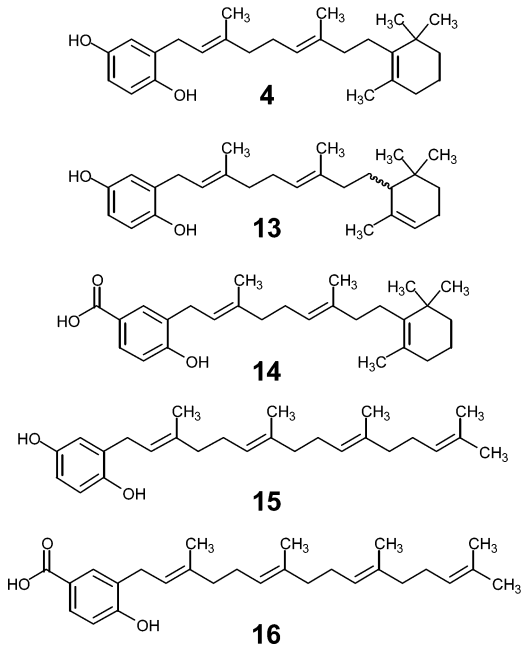

Figure 3. Group B: known marine-derived meroditerpenoids from Psammocinia sp. Jaspaquinol (**4**), cacospongin B (**13**), cacospongin D (**14**), 1,4-dihydroxy-2-tetraprenylbenzene (**15**), and 4-hydroxy-3-tetraprenylbenzoic acid (**16**).

HMBC and COSY NMR data were used to construct three partial structures, **A**−**C**, as illustrated in Figure 7. Substructure

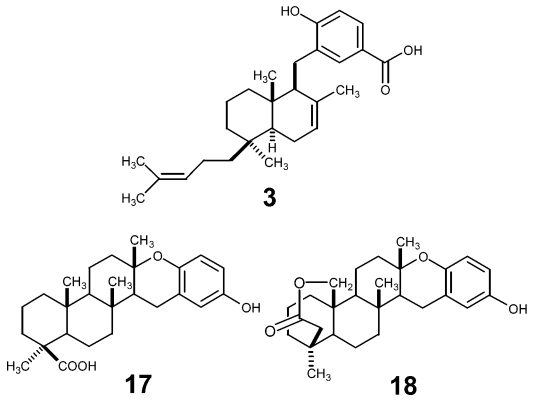

Figure 4. Group C: known marine-derived polycyclic meroditerpenoids jaspic acid (**3**) from *Psammocinia* sp. and strongylophorin-2 (**17**) and strongylophorin-3 (**18**) from *Strongylophorin* sp.

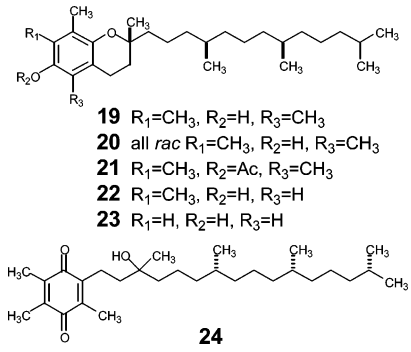

Figure 5. Group D: commercially available tocopherols (**19**−**24**).

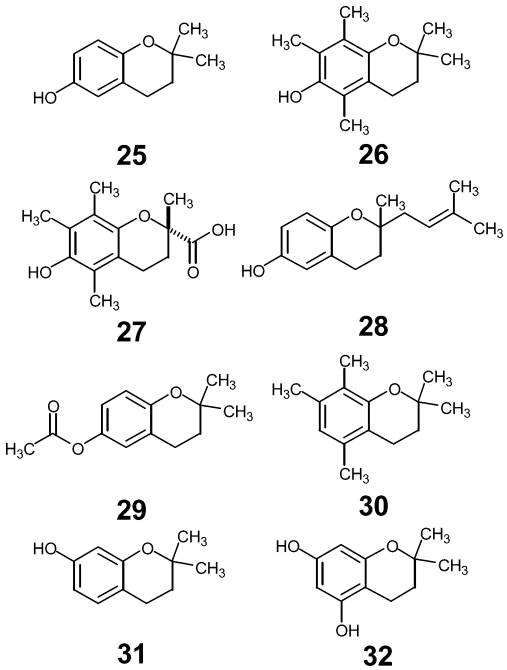

Figure 6. Group E: synthetic (**25**, **28**, **29**, **31**, and **32**) and commercial (**26**, **27**, and **30**) chromanes.

A contained all three of the oxygen-linked carbons as part of a 2-methyl-6-hydroxychromane moiety. Substructure **B** was composed of three sp^2 methines (δ_C 135.0, 126.0, 124.4), one quaternary sp^2 (δ_C 139.4), and one allylic methyl (δ_C 16.7), forming a butadiene moiety. The contiguously linked methine protons (δ_H 5.58, 6.73) were trans, as determined by their $^3J_{H,H}$ coupling ($^3J_{H-1',H-2'} = 15.5$ Hz). Furthermore, a trans $\Delta^{3'}$

Table 1. ^{1}H NMR Data (500 MHz, C_6D_6) for Chromarols A−E (**8**−**12**)

position	8	9	10	11	12
H-3	1.60 (m, 2H)	1.58 (m, 2H)	5.34 (d, J = 10.0 Hz, 1H)	5.34 (d, J = 10.0 Hz, 1H)	1.59 (m, 2H)
H-4$_a$	2.35 (ddd, J = 16.5, 5.0, 5.0 Hz, 1H	2.34 (ddd, J = 16.0, 5.0, 5.0 Hz, 1H)	6.11 (d, J = 10.0 Hz, 1H)	6.10 (d, J = 10.0 Hz, 1H)	2.20 (m, 1H)
H-4$_b$	2.56 (ddd, J = 16.5, 10.0, 6.5 Hz, 1H)	2.55 (ddd, J = 16.0, 10.0, 6.0 Hz, 1H)			2.42 (m, 1H)
H-5	6.33 (brs, 1H)	6.31 (d, J = 2.5 Hz, 1H)	6.27 (d, J = 3.0 Hz, 1H)	6.26 (d, J = 3.0 Hz, 1H)	8.00 (brs, 1H)
H-7	6.45 (brd, J = 8.5 Hz, 1H)	6.44 (dd, J = 8.5, 2.5 Hz, 1H)	6.33 (dd, J = 9.0, 3.0 Hz, 1H)	6.32 (dd, J = 8.5, 3.0 Hz, 1H)	8.11 (brd, J = 8.0 Hz, 1H)
H-8	6.99 (d, J = 8.5 Hz, 1H)	6.98 (d, J = 8.5 Hz, 1H)	6.81 (d, J = 9.0 Hz, 1H)	6.80 (d, J = 8.5 Hz, 1H)	6.99 (d, J = 8.0 Hz, 1H)
H-1′$_a$	5.58 (d, J = 15.5 Hz, 1H)	5.55 (d, J = 15.0 Hz, 1H)	1.81 (dd, J = 11.5, 5.5 Hz, 1H)	1.79 (dd, J = 11.0, 5.0 Hz, 1H)	5.44 (d, J = 15.0 Hz, 1H)
H-1′$_b$			1.67 (m, 1H)	1.66 (m, 1H)	
H-2′$_a$	6.73 (dd, J = 15.5, 11.0 Hz, 1H)	6.78 (dd J = 15.0, 11.0 Hz, 1H)	2.38 (m, 1H)	2.35 (m, 1H)	6.62 (dd, J = 15.0, 11.0 Hz, 1H)
H-2′$_b$				2.28 (m, 1H)	
H-3′	6.03 (brd, J = 11.0 Hz, 1H)	5.88 (d, J = 11.0 Hz, 1H)	5.33 (t, J = 7.0 Hz, 1H)	5.26 (t, J = 7.5 Hz, 1H)	6.01 (d, J = 11.0 Hz, 1H)
H-5′	2.19 (m, 2H)	2.25 (m, 2H)	2.21 (m, 2H)	2.12 (t, J = 8.0 Hz, 2H)	2.20 (m, 2H)
H-6′$_a$	2.19 (m, 2H)	2.11 (m, 2H)	2.25 (m, 2H)	1.68 (m, 1H)	2.20 (m, 2H)
H-6′$_b$				1.50 (m, 1H)	
H-7′				1.48 (m, 1H)	
H-9′	1.91 (t, J = 6.0 Hz, 2H)	1.93 (t, J = 6.5 Hz, 2H)	1.94 (t, J = 6.5 Hz, 2H)	5.38 (brt, J < 1.0 Hz, 1H)	1.91 (t, J = 6.0 Hz, 2H)
H-10′	1.60 (m, 2H)	1.58 (m, 2H)	1.62 (m, 2H)	2.01 (m, 2H)	1.47 (m, 2H)
H-11′$_a$	1.47 (m, 2H)	1.49 (m, 2H)	1.50 (m, 2H)	1.50 (m, 1H)	1.47 (m, 1H)
H-11′$_b$				1.13 (ddd, J = 13.0, 6.0, 3.0 Hz, 1H)	
C-13′	1.07 (s, 3H)	1.07 (s, 3H)	1.10 (s, 3H)	0.99 (s, 3H)	1.08 (s, 3H)
C-14′	1.07 (s, 3H)	1.11 (s, 3H)	1.10 (s, 3H)	0.98 (s, 3H)	1.08 (s, 3H)
C-15′	1.62 (s, 3H)	1.67 (s, 3H)	1.68 (s, 3H)	1.76 (s, 3H)	1.61 (s, 3H)
C-16′	1.67 (d, J = 1.0, 3H)	1.79 (s, 3H)	1.68 (s, 3H)	1.63 (s, 3H)	1.66 (s, 3H)
C-17′	1.43 (s, 3H)	1.42 (s, 3H)	1.34 (s, 3H)	1.33 (s, 3H)	1.33 (s, 3H)

Table 2. ^{13}C NMR Data (125 MHz, C_6D_6) for Chromarols A−E (**8**−**12**)

position	8	9	10	11	12
C-2	76.3 (s)	76.2 (s)	78.2 (s)	78.2 (s)	77.8 (s)
C-3	32.6 (t)	32.6 (t)	130.9 (d)	130.8 (d)	32.1 (t)
C-4	23.2 (t)	23.2 (t)	123.2 (d)	123.2 (d)	22.6 (t)
C-5	115.9 (d)	115.8 (d)	113.3 (d)	113.3 (d)	133.1 (d)
C-6	149.6 (s)	149.5 (s)	150.2 (s)	150.2 (s)	121.7 (s)
C-7	114.9 (d)	114.9 (d)	115.9 (d)	115.9 (d)	130.6 (d)
C-8	117.7 (d)	117.8 (d)	117.1 (d)	117.0 (d)	117.3 (d)
C-9	148.6 (s)	148.5 (s)	147.5 (s)	147.5 (s)	159.5 (s)
C-10	122.3 (s)	122.2 (s)	122.3 (s)	122.2 (s)	127.6 (s)
C-11					172.0 (s)
C-1′	135.0 (d)	135.0 (d)	41.5 (t)	41.5 (t)	134.0 (d)
C-2′	126.0 (d)	125.7 (d)	23.2 (t)	23.2 (t)	126.1 (d)
C-3′	124.4 (d)	125.4 (d)	124.2 (d)	124.6 (d)	124.1 (d)
C-4′	139.4 (s)	139.3 (s)	136.3 (s)	136.1 (s)	140.2 (s)
C-5′	40.9 (t)	33.6 (t)	40.9 (t)	41.0 (t)	40.9 (t)
C-6′	28.0 (t)	27.9 (t)	28.4 (t)	30.3 (t)	28.0 (t)
C-7′	137.2 (s)	137.3 (s)	137.4 (s)	49.4 (d)	137.1 (s)
C-8′	127.4 (s)	127.7 (s)	127.3 (s)	136.9 (s)	127.6 (s)
C-9′	33.1 (t)	33.2 (t)	33.1 (t)	120.4 (d)	33.1 (t)
C-10′	20.0 (t)	20.0 (t)	20.1 (t)	23.5 (t)	20.0 (t)
C-11′	40.3 (t)	40.3 (t)	40.3 (t)	32.1 (t)	40.2 (t)
C-12′	35.3 (s)	35.3 (s)	35.3 (s)	32.8 (s)	35.3 (s)
C-13′	28.8 (q)	28.9 (q)	28.9 (q)	27.7 (q)	28.8 (q)
C-14′	28.8 (q)	28.9 (q)	28.9 (q)	27.8 (q)	28.8 (q)
C-15′	20.0 (q)	20.2 (q)	20.1 (q)	23.7 (q)	20.0 (q)
C-16′	16.7 (q)	23.8 (q)	16.2 (q)	16.2 (q)	16.7 (q)
C-17′	27.8 (q)	27.9 (q)	26.3 (q)	26.3 (q)	27.7 (q)

configuration was deduced on the basis of the relative upfield shift of the C-4′ methyl.[12] This configuration for substructure **B** was supported by difference NOE experiments in which

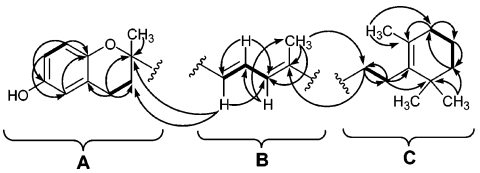

Figure 7. Partial structures **A**−**C** for chromarol A (**8**). Significant $^{2-3}J_{H-C}$ HMBC and ^{1}H−^{1}H COSY correlations are represented as arrows and bold bonds, respectively.

irradiation of H-1′ yielded a large enhancement of H-3′, while irradiation of H-2′ gave a significant enhancement of the H_3-16′ signal. The remaining protons and carbons were recognized as a 1,3,3-trimethyl-2-alkylcyclohex-1-ene moiety on the basis of comparisons with NMR shifts reported for jaspaquinol[13] (**4**) and confirmed by HMBC data. With partial structures **A**−**C** identified, HMBC data were used to link these substructures together. It was observed that H-1′ of substructure **B** exhibited $^{2-3}J_{H,C}$ coupling with C-2 and C-3 in **A**. In contrast, H_3-16′ methyl protons were coupled ($^3J_{H,C}$) to the C-5 methylene in substructure **C**, while the H-5 protons were coupled ($^2J_{H,C}$) to C-4′ in fragment **B**. Thus, the planar structure of chromarol A (**8**) was established as a new chromane meroditerpene.

Comparisons of the MS and NMR data of **8** and chromarol B (**9**) indicated that they were closely related. In fact, only the δ_C shifts of C-5′ (33.6 t) and C-16′ (23.8 q) were found to vary significantly, suggesting that **9** was an isomer of **8**. Focusing on the diagnostic downfield shift of the C-16′ methyl, it was apparent that **9** possessed a different, cis $\Delta^{3'}$ configuration. This was confirmed by difference NOE experiments in which

(12) Crews, P.; Rodriguez, J.; Jaspars, M. *Organic Structure Analysis*;Oxford University Press: New York, 1998.

(13) Murray, L. M.; Johnson, A.; Diaz, M. C.; Crews, P. *J. Org. Chem.* **1997**, *62*, 5638−5641.

Table 3. Experimental and Literature CD Data for Chromarols and Chromanes

CD spectra (EtOH) of compounds **8**, **10**, and **21**[a]	structure	Cotton effect sign (260–295 nm)
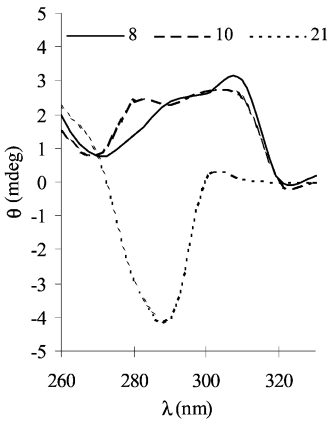	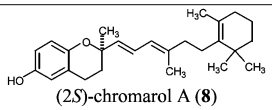 (2*S*)-chromarol A (**8**)	+
	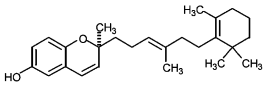 (2*R*)-chromarol C (**10**)	+
	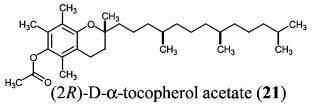 (2*R*)-D-α-tocopherol acetate (**21**)	−
	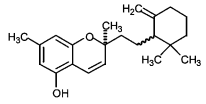 (2*S*)-siccanochromene-A (**33**)	+[b]
	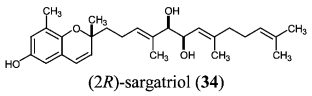 (2*R*)-sargatriol (**34**)	−[c]

[a] CD spectra for compounds **9**, **11**, and **12** exhibited Cotton effects similar to those shown for **8** and **10**. A summary of these results is given in the Experimental Section. [b] Reported in ref 16. [c] Reported in ref 17.

irradiation of H-3′ yielded significant enhancements of the H-1′ and H_3-16' signals, while irradiation of H-2′ provided a large enhancement of H_2-5′.

Chromarols C (**10**) and D (**11**) both exhibited the same molecular formulas as **8** and **9**, but the ^{1}H and ^{13}C NMR data revealed that fragments **A** and **B** were modified. Assignment of the low-field ^{13}C spins in **10** and **11** showed that fragment **A** was now a chromene, as indicated by the relative downfield shifts of C-3 and C-4 (Table 2). Furthermore, two new upfield C-1′ and C-2′ sp^3 methylenes were observed in fragment **B** of **10** and **11**. Analysis of the C-16′ methyl shifts for **10** and **11** showed that they exhibited the same trans $\Delta^{3'}$ configuration as in **8**. Fragment **C** in compound **10** was recognized as identical to that found in **4**. In contrast, fragment **C** in compound **11** showed evidence of a positional change in the C-7′ olefin identical to that reported for **13**. This was further confirmed by HMBC experiment, providing confirmation for the planar structure of **11**.

Analysis of compound **12** by HRESIMS revealed an ion at *m*/*z* 409.2742 $[M + H]^+$ (calcd 409.2743) that supported a molecular formula of $C_{27}H_{36}O_3$. Compared to **8**, compound **12** possessed one additional carbon and one additional oxygen. In view of the low-field shift of the new carbon resonance (δ_C 172.0) and upfield shift of C-6 (δ_C 121.7) in **12**, a carboxylic acid functionality was rationalized in place of the 6-hydroxyl moiety found in **8**. The ^{1}H and ^{13}C NMR shifts of substructures **B** and **C** in **12** were identical to those in **8**, revealing the shared architecture of the two compounds. These similarities were subsequently confirmed by HMBC data, thus corroborating the planar structure for **12**.

With the planar structures of **8**−**12** identified, attention was focused on defining the C-2 absolute configuration of these new metabolites. Compounds **8**−**12** all exhibited positive [α] values, suggesting that the chromarols shared an identical stereochemistry at the C-2 chiral center. However, these data did not help in determining the C-2 configuration, since the sign and magnitude of [α] values of chiral chromanes have been shown to be highly variable and solvent dependent.[14,15] In contrast, the circular dichroism (CD) spectra of **8**−**12** proved invaluable in addressing this issue. In previous applications of helicity rules to chromane derivatives, the sign of the Cotton effect between 260 and 295 nm was determined to be reflective of the C-2 absolute configuration.[16−18] For example, a positive Cotton effect between 277 and 289 nm was critical in discerning the absolute configuration of the plant-derived (2*S*)-siccanochromene-A[16] (**33**). In contrast, a distinct negative Cotton effect from 265 to 275 nm was key in assigning an opposite absolute C-2 stereochemistry for the algal-derived chromene (2*R*)-sargatriol[17] (**34**). Likewise, a negative Cotton effect (289 nm) was observed for the standard (2*R*)-D-α-tocopherol acetate (**21**), which was identical to that previously reported for this compound.[15] These data are summarized in Table 3. As further shown in Table 3, positive Cotton effects were observed for chromarols **8** and **10**. Similar positive Cotton effects were also obtained for **9**, **11**, and **12**. Accordingly, a 2*R* configuration is assigned to chromanes **8**, **9**, and **12**, while a 2*S* absolute stereochemistry is attributed to chromenes **10** and **11**. The C-7′ configuration of **11** could not be ascertained on the basis of the available data. However, the major ring **C** conformation must be with the side chain equatorial.

While the occurrence of meroterpenes is common among marine organisms, the presence of chromane derivatives is notably more restricted. For example, chromane meroterpenoids

(14) Schudel, P.; Mayer, H.; Metzger, J.; Rüegg, R.; Isler, O. *Helv. Chim. Acta* **1963**, *46*, 333−343.
(15) Sur, S.; Colpa, J. P. *Chem. Phys. Lett.* **1986**, *127*, 577−580.
(16) Nozoe, S.; Hirai, K.; Snatzke, F.; Snatzke, G. *Tetrahedron* **1974**, *30*, 2773−2776.
(17) Kikuchi, T.; Mori, Y.; Yokoi, T.; Nakazawa, S.; Kuroda, H.; Masada, Y.; Kitamura, K.; Kuriyama, K. *Chem. Pharm. Bull.* **1983**, *31*, 106−113.
(18) Antus, S.; Kurtan, T.; Juhasz, L.; Kiss, L.; Hollosi, M.; Majer, Z. S. *Chirality* **2001**, *13*, 493−506.

Scheme 1

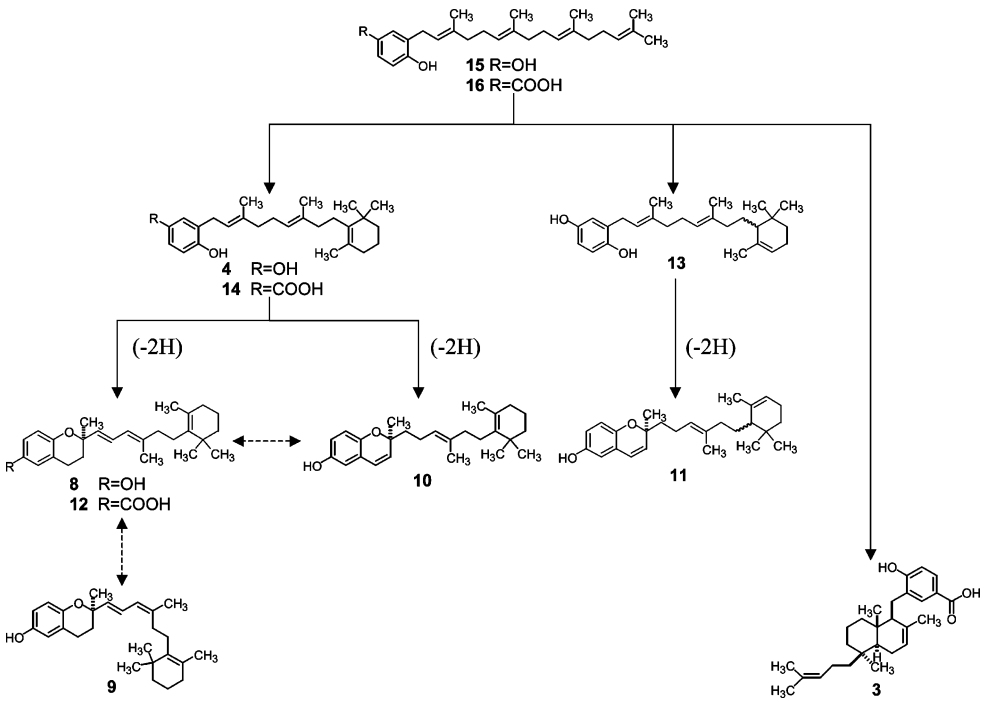

were reported from the brown algae *Sargassum tortile*,[17,19] *Cystoseira* sp.,[20] and *Dictyopteris unulata*[21] as well as the green calcareous alga, *Cymopolia barbata*.[22] Further reports of marine invertebrate-derived chromanes include their isolation from ascidians in the genus *Aplidium*[23] and the sponges *Halichondria pancicea*,[24] *Haliclona* sp.,[25] *Reniera fulva*,[26] and *Reniera mucosa*.[27] Interestingly, unlike **8**−**12**, many of these other chromanes, co-isolated with their putative linear meroterpene precursors, were obtained as mixtures of C-2 isomers, which raises questions about the final steps in their biosynthesis.

Compounds **8**−**12** are intriguing in light of the co-isolation of their probable biogenic precursors from *Psammocinia*. For example, cyclization of the linear meroditerpenoids **15** and **16** would furnish the monocyclic **4**, **13**, and **14** and polycyclic **3** as illustrated in Scheme 1. A second cyclization event with the concomitant dehydration of **4**, **13**, and **14** would yield chromarols **8** and **10**−**12**. Finally, isomerization of the (1′*E*,3′*E*)-diene in **8** could generate (1′*E*,3′*Z*)-**9**. The presence of enatiomericaly pure C-2 isomers **8**−**12** suggests that this cyclization is enzymaticly controlled and not the result of an acid-mediated process.[23b]

In an analogous case, the synthesis of tocopherols (Figure 5) by plants and cyanobacteria[28] is attributed to tocopherol cyclase.[29] This enzyme catalyzes the intramolecular chromane ring formation step between the phenolic headgroup and phytyl tail via double bond *si* protonation, with the concomitant *re* attack by the phenolic oxygen. It is conjectured that a different enzyme is required for cyclization of chromarols **8**−**12** since all known tocopherol cyclases catalyze the formation of products bearing the opposite C-2 absolute configuration and require a 1,4-dihydroquinone moiety for cyclization to occur.[29] In addition to the opposite C-2 sterochemistry of **8**−**12** compared to natural tocopherols, compound **12** is speculated to have arisen from the 4-hydroxybenzoic acid precursor compound **14**, whose carboxyl-bearing aromatic headgroup would not serve as an appropriate substrate for tocopherol cyclase. Interestingly, this is the first report of a natural marine-derived chromane bearing a stereochemistry opposite to that of the natural (2*R*)-tocopherols.

Biological Evaluation of Groups A−C: Marine-Derived Meroditerpenes. The group A compounds (Figure 2) were tested in order to determine their comparative inhibition against 15-hLO and 12-hLO. The results of this analysis are shown in Table 4. These data were quite remarkable, with chromarols A−D (**8**−**11**) exhibiting selective (>25−166-fold) inhibition against 15-hLO versus 12-hLO. Furthermore, **8**−**11** were relatively potent inhibitors of 15-hLO, exhibiting IC_{50} values ranging from 0.6 ± 0.1 to 4.0 ± 0.5 μM. In stark contrast, the 6-carboxychromane derivative, chromarol E (**12**), exhibited no selectivity for either isozyme. Instead, **12** displayed comparable potency against both 15-hLO and 12-hLO ($IC_{50} = 3.3 \pm 0.4$ and 1.2 ± 0.1 μM, respectively).

The acyclic and monocyclic *Psammocinia*-derived meroditerpenes (**4** and **13**−**16**) constituting group B are shown in Figure 3. An examination of their inhibitory effects against 15-hLO and 12-hLO revealed a very different activity profile for these

(19) (a) Kato, T.; Kumanireng, A. S.; Ichinose, I.; Kitahara, Y.; Kakinuma, Y.; Kato, Y. *Chem. Lett*. **1975**, 335−338. (b) Ishitsuka, M.; Kusumi, T.; Nomura, Y.; Konno, T.; Kakisawa, H. *Chem. Lett*. **1979**, 1269−1272. (c) Numata, A.; Kanbara, S.; Takahashi, C.; Fujiki, R.; Yoneda, M.; Usami, Y.; Fujita, E. *Phytochemistry* **1992**, *31*, 1209−1213.
(20) Navarro, G.; Fernandez, J. J.; Norte, M. *J. Nat. Prod.* **2004**, *67*, 495−499.
(21) Dave, M.-N.; Kusumi, T.; Ishitsuka, M.; Iwashita, T.; Kakisawa, H. *Heterocycles* **1984**, *22*, 2301−2307.
(22) Hogberg, H.-E.; Thomson, R. H.; King, T. J. *J. Chem. Soc., Perkin Trans. 1* **1976**, 1696−1701.
(23) (a) Kim, I. K.; Erickson, K. L. *Magn. Reson. Chem*. **1993**, *31*, 788−789. (b) Rochfort, S. J.; Metzger, R.; Hobbs, L.; Capon, R. J. *Aust. J. Chem*. **1996**, *49*, 1217−1219. (c) Garrido, L.; Zubía, E.; Ortega, M. J.; Salvá, J. *J. Nat. Prod*. **2002**, *65*, 1328−1331.
(24) Cimino, G.; De Stefano, S.; Minale, L. *Tetrahedron* **1973**, *29*, 2565−2570.
(25) Jaspars, M.; Horton, P. A.; Madrid, L. H.; Crews, P. *J. Nat. Prod*. **1995**, *58*, 609−612.
(26) Casapullo, A.; Minale, L.; Zollo, F. *J. Nat. Prod*. **1993**, *56*, 527−533.
(27) Zubía, E.; Ortega, M. J.; Carballo, J. L.; Salvá, J. *Tetrahedron* **1994**, *50*, 8153−8160.
(28) Sattler, S. E.; Cahoon, E. B.; Coughlan, S. J.; DellaPenna, D. *Plant Physiol*. **2003**, *132*, 2184−2195.
(29) Stocker, A.; Fretz, H.; Frick, H.; Rüttimann, A.; Woggon, W.-D. *Bioorg. Med. Chem*. **1996**, *4*, 1129−1134.

Table 4. Inhibitory Effects of Compounds **3**, **4**, and **8**−**32** against Lipoxygenases

compound	$IC_{50} \pm SE$ (μM) 15-hLO	12-hLO	redox active	cLog *P*[a]
	Group A: Marine-Derived Chromarols			
8	0.6 ± 0.1	>100	yes	8.0
9	4.0 ± 0.5	>100	yes	8.0
10	0.7 ± 0.08	>100	yes	8.0
11	1.1 ± 0.2	>100	yes	8.0
12	3.3 ± 0.4	1.2 ± 0.1	no	8.2
	Group B: Marine-Derived Meroterpenoids			
4	0.3 ± 0.1	4.5 ± 1.0	yes	8.1
13	3.1 ± 1.0	0.7 ± 0.09	yes	8.2
14	2.4 ± 0.3	4.0 ± 0.4	no	8.5
15	2.3 ± 0.6	0.6 ± 0.06	yes	8.1
16	0.8 ± 0.09	1.6 ± 0.2	no	8.5
	Group C: Marine-Derived Polycyclic Meroterpenoids			
3	1.4 ± 0.2	0.7 ± 0.05	no	8.5
17	44.6 ± 5.0	>70	yes	6.5
18	14.7 ± 2.0	>70	yes	6.5
	Group D: Tocopherols			
19	>60	>100	nd[b]	11.0
20	>60	>100	nd	11.0
21	>60	>100	nd	11.1
22	>60	>100	nd	10.5
23	>60	>100	nd	10.1
24	>60	>100	nd	8.9
	Group E: Synthetic Chromanes			
25	11.8 ± 0.8	>100	yes	2.8
26	0.3 ± 0.04	>100	yes	4.3
27	4.7 ± 0.8	>100	nd	3.1
28	0.4 ± 0.09	>100	yes	4.6
29	>100	>100	nd	4.6
30	>100	>100	nd	2.8
31	11.1 ± 0.8	12.1 ± 0.9	nd	2.8
32	>100	>100	nd	2.3
	Standard			
NDGA	0.11 ± 0.01	5.1 ± 1.0	yes	3.9

[a] cLog *P* calculations were performed using CLOGP: Daylight Chemical Information Systems, Inc. (http://www.daylight.com/daycgi/clogp), and ChemDraw version 6.0: CambridgeSoft. [b] nd, not determined.

compounds compared to the group A metabolites. Remarkably, compounds **4**, **13**, and **15**, the putative direct biogenic precursors of **8**−**11** (see Scheme 1), showed no selection against either 15-hLO or 12-hLO, but retained potent inhibitory activities against both isozymes. For example, compound **15** exhibited IC_{50} values of 2.3 ± 0.6 and 0.6 ± 0.06 μM against 15-hLOand 12-hLO, respectively. Among the group B derivatives, substitution of a carboxylic acid (i.e., compound **16**) for the phenolic hydroxyl moiety caused no significant change in potency or selectivity against both 15-hLOand 12-hLO. This is in contrast to the change in activity profile observed for the group A chromarols. Furthermore, it can be deduced from this data set that the presence or absence of the cyclohexene moiety found in **4**, **13**, and **14** versus acyclic metabolites **15** and **16** had no discernible influence on selectivity or potency.

The next set of compounds investigated for hLO inhibitory effects were the group C marine-derived polycyclic meroditerpenes (Figure 4). Similar to our previous findings, compound **3** exhibited potent but nonselective activity against 15-hLO (1.4 ± 0.2 μM) and 12-hLO (0.7 ± 0.05 μM). In contrast, the hypercyclized meroditerpenes **17** and **18** exhibited modest but selective inhibitory activity only against 15-hLO (44.6 ± 5.0 and 14.7 ± 2.0 μM for **17** and **18**, respectively).

At this point in the study, it was important to summarize the structure−activity trends that arose regarding the chemical features that conveyed potent and selective inhibition of 15-hLO. The acyclic dihydroquinone (**15**) and 4-hydroxybenzoic acid (**16**) meroditerpenes are potent inhibitors and represent core structures upon which further modifications can be made to improve selectivity. For example, replacement of the phenolic headgroup with a chromane moiety, such as in compounds **8**−**11**, yielded highly potent and 15-hLO-selective inhibitors. However, substitution of a carboxylic acid for the 6-hydroxyl group, as seen in compound **12**, eliminated selectivity for 15-hLO. Comparison of compounds **8**−**11** suggests that the isoprene side chain offered a flexible region for structure modification of the group A-type inhibitors; however, certain limitations to this may exist. For example, compounds **17** and **18**, in which a chromane moiety is fused to a hypercyclized diterpene skeleton, still retained selectivity for hLO-15 but were approximately 20-fold less active. On the basis of these observations, the 6-hydroxychromane moiety present in **8**−**11** emerged as a pertinent target for further investigation. Therefore, the next step involved testing this hypothesis against other available scaffolds containing the 6-hydroxychromane pharmacophore.

Biological Evaluation of Group D: Tocopherols. A review of the literature regarding chromane-containing lipoxygenase inhibitors revealed that the tocopherols were relevant to consider further. For example, several tocopherols were previously reported as inhibitors of 15-soybean lipoxygenase (15-sLO)[30] and 5-potato lipoxygenase (5-pLO).[31,32] With this in mind, tocopherols (**19**−**23**) and D-α-tocopherol quinone (**24**) were screened against 15-hLO and 12-hLO. Interestingly, none of the group D tocopherols shown in Figure 5 exhibited any inhibitory effects at the concentrations listed in Table 4. We suspect that the greater hydrophobicity of the tocopherols (cLog *P* values ≥ 8.9, Table 4) had a significant impact on their inaccessibility to the enzyme active site, which has been shown to play a significant role in hLO inhibitor potency.[33]

Biological Evaluation of Group E: Synthetic Chromanes. Next, a panel of eight chromane derivatives (**25**−**32**, Figure 6) devoid of a diterpenoid side chain was evaluated. Compounds **26**, **27**, and **30** were commercially available; however, the remaining chromanes were prepared according to the method of Kalena et al.,[34] in which a catalytic, acidic solid-phase cation-exchange resin facilitated the condensation of isoprene with various phenols, yielding the chromane derivatives illustrated in Scheme 2. The structures of the synthetic chromanes were confirmed by HRESIMS and NMR. The biological activities of these chromanes provided significant insight into the structure−activity requirements for the potent and selective inhibition of 15-hLO.

The 6-hydroxychromanol **25** and its pentamethyl congeners **26** and **27** both exhibited selective inhibition against 15-hLO; however, **25** was less potent (IC_{50} = 11.8 ± 0.8 μM) than **26** (IC_{50} = 0.3 ± 0.04 μM) and **27** (IC_{50} = 4.7 ± 0.8 μM). On the basis of the indication that the 6-hydroxychromane moiety

(30) Grossman, S.; Waksman, E. G. *Int. J. Biochem.* **1984**, *16*, 281−289.
(31) Reddanna, P.; Rao, M. K.; Reddy, C. C. *FEBS* **1985**, *193*, 39−43.
(32) Cucurou, C.; Battioni, J. P.; Daniel, R.; Mansuy, D. *Biochim. Biophys. Acta* **1991**, *1081*, 99−105.
(33) Eleni, P.; Dimitra, H.-L. *Mini Rev. Med. Chem.* **2003**, *3*, 487−499.
(34) Kalena, G. P.; Jain, A.; Banerji, A. *Molecules* **1997**, *2*, 100−105.

Scheme 2

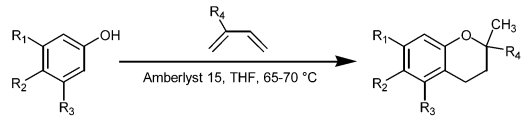

35 R_1=H, R_2=OH, R_3=H, R_4=CH_3

36 R_1=OH, R_2=H, R_3=OH, R_4=CH_3

37 R_1=OH, R_2=H, R_3=H, R_4=CH_3

38 R_1=H, R_2=OH, R_3=H, R_4= 

25 R_1=H, R_2=OH, R_3=H, R_4=CH_3

32 R_1=OH, R_2=H, R_3=OH, R_4=CH_3

31 R_1=OH, R_2=H, R_3=H, R_4=CH_3

28 R_1=H, R_2=OH, R_3=H, R_4= 

played a significant role in 15-hLO inhibition, acetate **29** and dehydroxylated compound **30** were examined. Both compounds were completely inactive, supporting the conclusion of the necessity of the 6-hydroxyl moiety. The role and positional effects of the 6-hydroxyl were further investigated by testing the inhibitory activities of the 7-hydroxychromanol derivative **31** and dihydroxyresorcinol product **32**. The monophenolic **31** exhibited equivalent potency against 15-hLO (IC_{50} = 11.1 ± 0.8 μM) and 12-hLO (IC_{50} = 12.1 ± 0.9 μM). In striking contrast, compound **32** was completely inactive against both 15-hLO and 12-hLO. Interestingly, compared to **25**, chromane **28**, possessing an isoprene tail, exhibited improved potency against 15-hLO (IC_{50} = 0.4 ± 0.09 μM) versus 12-hLO (IC_{50} ≥ 100 μM). This pattern was similar to the activity profiles observed for **8**−**11**. It appears that the isoprene tail on **28** contributed to improved potency due to enhanced active-site binding interactions or more favorable hydrophobicity properties,[32] in a manner analogous with the larger diterpene units present on **8**−**11**. This point is further supported by the appreciably greater potency exhibited by the more hydrophobic pentamethylated chromane **26** as opposed to **25**.

In summary, several important features were identified that appear to significantly influence the potency and selectivity of these 15-hLO inhibitors. First, a 6-hydroxychromane moiety is essential for both potency and selectivity against 15-hLO compared to 12-hLO. Second, the position of the hydroxyl group is crucial for selectivity. Third, the hydrophobicity (clog *P* values) of the chromanes may contribute to the potency of these inhibitors.

Evaluation of the 6-Hydroxychromanol Mode of Action against Lipoxygenases. The inactive, native form of lipoxygenase possesses a non-heme ferrous center in its active site. Activation of lipoxygenase involves oxidation of the iron to the ferric species. Compounds such as the nonselective redox inhibitor, nordihydroguarierate acid (NDGA) (see Table 4), inactivate lipoxygenase by reducing the activated ferric center. However, many of these types of inhibitors can suffer from shortcomings, including in vivo inactivation via competing oxidation pathways or toxicity of the oxidized/free radical intermediates.[35]

Compounds **3**, **4**, **8**−**18**, **25**, **26**, and **28** were tested to determine if they might act as redox inhibitors of lipoxygenase via reduction of the active-site ferric iron (Table 4). We have previously reported on the use of a simple and rapid fluorescence-based assay utilizing 15-soybean lipoxygenase (15-sLO), an enzyme homologous to 15-hLO, as a reliable method for the determination of inhibitor redox activity against lipoxygenases in general.[5,6] Compounds **4**, **8**−**11**, **13**, **15**, **17**, **18**, **25**, **26**, and

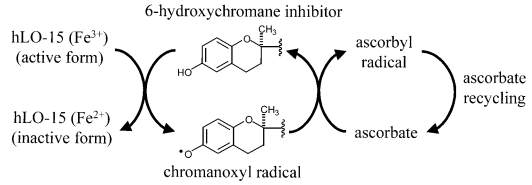

Figure 8. Proposed chromanoxyl radical recycling scheme for chromarols and synthetic chromanes.

28, possessing 6-hydroxychromanes, functioned as potent reducing agents of the lipoxygenase non-heme ferric center, and as a result, these 6-hydroxychromanes can be classified as redox inhibitors. Previous studies have shown that structurally similar 6-hydroxychromanes act as potent reducing agents through the formation of a chromanoxyl radical species.[36] The oxidative processes associated with chromanoxyl radical formation from 6-hydroxychromanols have been well studied by numerous methods with tocopherols and tocopherol mimetics.[36,37] Interestingly, these studies suggest a recyclable regeneration mechanism for the oxidized chromanoxyl radical species in vitro and in vivo.[36,38,39] Regeneration of the 6-hydroxychromane moiety is dependent upon the ubiquitous antioxidant, ascorbate, that readily reduces the chromanoxyl radical.[40] Importantly, ascorbate itself is also recycled in vivo, thereby providing for the continued regeneration of the 6-hydroxychromane.[41]

We propose that the group A chromarols and group E synthetic 6-hydroxychromanes can undergo a parallel transformation process upon inactivation of 15-hLO as illustrated in Figure 8. This hypothesis was supported by an initial observation that the potency of chromanol **25** against 15-hLO, as determined by a depression in the IC_{50} value, was significantly improved (i.e., 3-fold reduction) in the presence of 0.5 mM ascorbate in the incubation buffer (15-hLO IC_{50} = 3.9 ± 0.5 μM). Ascorbate itself has no measurable effect on enzyme activity at this concentration (15-hLO IC_{50} > 1000 μM). While this observation was intriguing, it did not provide exclusive support for our hypothesis. To investigate this concept further, a fluorescence-based assay using 15-sLO was utilized to study the redox recycling of 6-hydroxychromanes by ascorbate.

In this fluorescence-based study (see Experimental Section), we observed that 1 molar equiv of 13-hydroperoxy-9(*Z*),11(*E*)-octadecadienoic acid (HPOD) was required to completely oxidize the 15-sLO active-site ferrous iron and that 1 equiv of chromane **26** was sufficient to completely reduce the lipoxygenase ferric iron. The ferrous iron was subsequently reoxidized by the further addition of 1 equiv of HPOD to the incubation buffer because the 1 equiv of chromane **26** had been oxidized.

This study was repeated, but this time ascorbate (1 equiv) was added at the outset to the incubation buffer. Under these conditions, the initial addition of 1 equiv of HPOD completely oxidized the 15-sLO ferrous iron. Again, the addition of 1 equiv

(35) McMillan, R. M.; Walker, E. R. H. *Trends Pharmacol. Sci.* **1992**, *13*, 323−330.

(36) Guo, Q.; Packer, L. *Free Radical Biol. Med.* **2000**, *29*, 368−374.
(37) Kagan, V. E.; Serbinova, E. A.; Forte, T.; Scita, G.; Packer, L. *J. Lipid Res.* **1992**, *33*, 385−397.
(38) Kagan, V. E.; Kuzmenko, A. I.; Shvedova, A. A.; Kisin, E. R.; Li, R.; Martin, I.; Quinn, P. J.; Tyurin, V. A.; Tyurina, Y. Y.; Yalowich, J. C. *Biochim. Biophys. Acta* **2003**, *1620*, 72−84.
(39) Halpner, A. D.; Handelman, G. J.; Harris, J. M.; Belmont, C. A.; Blumberg, J. B. *Arch. Biochem. Biophys.* **1998**, *359*, 305−309.
(40) Gorbunov, N. V.; Osipov, A. N.; Sweetland, M. A.; Day, B. W.; Elsayed, N. M.; Kagan, V. E. *Biochem. Biophys. Res. Commun.* **1996**, *219*, 835−841.
(41) Kagan, V. E.; Shvedova, A.; Serbinova, E.; Khan, S.; Swanson, C.; Powell, R.; Packer, L. *Biochem. Pharm.* **1992**, *44*, 1637−1649.

of chromane **26** reduced the activated iron to the ferrous species. However, unlike before, the further addition of 1 equiv of HPOD failed to permanently reoxidize the 15-sLO active-site iron. This was witnessed as a brief initial oxidation of the 15-sLO, followed by its immediate and complete reduction due to the regeneration of chromane **26** by ascorbate following reduction of ferric iron. This experiment supports the hypothesis that the chromanoxyl radical generated via reduction of the 15-sLO ferric species was regenerated (reduced) by ascorbate. Interestingly, under conditions in which ascorbate was withheld from the incubation medium until after the addition of 2 equiv of HPOD and 1 equiv of **26** to the enzyme, only a partial reduction of the lipoxygenase occurred. This is likely due to the time-dependent irreversible oxidative transformation of the chromanoxyl radical to a quinone species. Taken together, the evidence from both the 15-hLO chromane−ascorbate co-incubation study, combined with the results from the 15-sLO fluorescence experiement, supports the existence of a regeneration pathway for 6-hydroxychromanes in the presence of ascorbate that could also potentially occur in vivo.

Summary. In light of the contributory role of 15-hLO to atherogenic processes, potent and selective inhibitors of this enzyme are needed. Previous collaborative studies between our laboratories have demonstrated that marine sponges can serve as a valuable source of novel hLO inhibitors. In this investigation, the new meroditerpenes, chromarols A−D (**8**−**11**) from *Psammocinia* sp., were discovered as potent and selective inhibitors of 15-hLO versus 12-hLO. On the basis of this research, the 6-hydroxychromane moiety was identified as a key pharmacophore for the further development of selective 15-hLO inhibitors. It was demonstrated that the 6-hydroxychromane 15-hLO inhibitors function via a redox mechanism. More importantly, these compounds can be regenerated by ascorbate through a redox-recycling pathway. Thus, 6-hydroxychromanes represent a unique series of 15-hLO inhibitors that deserve further attention as lead compounds for development as novel agents for the treatment of atherosclerosis.

Experimental Section

General Methods. All 1D- and 2D-NMR spectra were recorded in C_6D_6 (Cambridge Isotope Laboratories, Inc.) on Varian UNITY INOVA 500 instruments. Electrospray mass spectral data were obtained on an Applied Biosystems Mariner Biospectrometry Workstation. The optical rotations were determined on a Jasco DIP 370 polarimeter.

Silica gel (230−400 mesh) was obtained from Fischer. Analytical and preparative thin-layer chromatography was performed on Macherey-Nagel Polygram G/UV_{254} and Analtech Uniplates (1000 μm) plates, respectively. Sephadex LH-20 was obtained from Sigma-Aldrich. Preparative HPLC was carried out on a Waters 600E system controller and pumps with a Prep LC 25 mm radial compression column using 25 × 100 mm C_{18} Nova-Pak HR18 (6 μm) cartridges. Peak detection utilized a Sedex 55 light-scattering detector and a Pharmacia LKB UV-1 (254 nm) detector. Semipreparative HPLC was performed on a C_{18} Phenomenex 10 × 250 mm Synergi Hydro-RP (4μm) column with Waters 510 HPLC pumps and gradient controller and with a Waters 484 tunable absorbance detector (210 nm). All HPLC solvents were of HPLC quality, while all other solvents were of ACS grade (EMD Chemicals). All other chemicals, including the tocopherols (**19**−**24**), selected chromanes (**26**, **27**, and **30**), linoleic acid, arachidonic acid, Amberlyst resin, and synthetic precursors, were obtained from Sigma-Aldrich and used without further purification.

Animal Material. The sponge (UCSC collection number 01236) was collected by SCUBA from the Madang region of Papua New Guinea in 2001. The sponge (~1 kg wet weight) exhibited a compressible, globular (3−8 cm) morphology with a grayish to dark brown exterior and tan interior. The surface of the organism was covered with sharp conules 1 mm in length and spaced approximately 2−4 cm apart. Round, compound oscules were observed (1−2 per specimen) on the sponge surface. The skeleton of the animal was composed of an irregular reticulation of strongly laminated fibers with sporadic, stout primary fibers (250−600 μm diameter) and thinner, irregularly spaced secondary fibers (100−180 μm diameter) forming a loose fascicular reticulation. The cortex of the sponge contained large quantities of foreign matter consisting of spicules and sediments. In addition to the sandy mesophyl, the sponge was distinguished by a low abundance of filaments with a flattened morphology that lacked knobby ends. These features indicate that UCSC 01236 is an undescribed species of *Psammocinia* (Dictyoceratida, Irciniidae). The *Psammocinia* sp. utilized in these studies was characterized as morphologically distinct from that reported in our previous disclosure.[10] Immediately following collection, the sponge was soaked in EtOH−sea H_2O (1:1) for 24 h, after which the liquid was decanted and the sponge transported to UCSC. Upon arrival, the sponge was immediately immersed in MeOH and placed in cold storage at 4 °C until extracted. A voucher specimen has been retained at UCSC for reference.

Extraction and Isolation of Natural Products. The sponge material (UCSC collection number 01236) was extracted with MeOH (1.5 L × 3), and the combined extracts were submitted to solvent−solvent partitioning with hexane. Additional H_2O was added to the MeOH-soluble portion (1:1, v/v) and extracted with CH_2Cl_2 (×3). The aqueous MeOH portion was further diluted with H_2O (9:1, v/v) and extracted with butanol (×3). The butanol-soluble portion (3 g) exhibited potent 15-hLO inhibitory activity and was selected for bioactivity-guided isolation.

The active butanol-soluble extract was applied to Sephadex LH-20 (MeOH), providing four fractions. The third fraction (1.4 g) retained the 15-hLO inhibitory activity and was further divided by preparative HPLC (C_{18}, 70−100% CH_3CN), giving eight fractions. Fraction five (15 mg) was purified by semipreparative HPLC (80−100% CH_3CN), yielding 6 mg of chromarol B (**9**). Preparative HPLC fraction six (20 mg) was applied to PTLC (SiO_2) with toluene−2-propanol (30:1), providing 11 mg of chromarol A (**8**). Preparative HPLC fraction seven (14 mg) was repeatedly subjected to semipreparative HPLC (83% CH_3CN), giving 1 mg of chromarol E (**12**). Preparative HPLC fraction eight (67 mg) was further purified by PTLC (CH_2Cl_2−CH_3CN, 40:1), providing two fractions. Fraction one (30 mg) was subjected to repeated semipreparative HPLC (89% CH_3CN), yielding 6 mg of chromarol C (**10**) and 5 mg of chromarol D (**11**). The remaining preparative HPLC fractions one through four were purified by PTLC and HPLC to give the known compounds **3**,[13] **4**,[13] **13**,[42] **14**,[43] **15**,[43] and **16**[44] that were identified by comparison to literature data. Compounds **17** and **18** were previously obtained from *Strongylophora* sp. (UCSC collection number 02139) by HPLC. The structures were verified by comparisons to published spectroscopic data.[44]

Chromarol A (8): clear oil; $[\alpha]^{27}_D = 17°$ (*c* 0.17, EtOH); CD (EtOH) 294 ($\Delta\epsilon$ 2.5), 300 ($\Delta\epsilon$ 2.6); ^{1}H NMR data see Table 1; ^{13}C NMR data see Table 2; HRESIMS *m*/*z* 381.2796 $[M + H]^+$ (calcd for $C_{26}H_{37}O_2$ 381.2794) and 403.2615 $[M + Na]^+$ (calcd for $C_{26}H_{36}O_2Na$ 403.2613).

Chromarol B (9): clear oil; $[\alpha]^{27}_D = 14°$ (*c* 0.17, EtOH); CD (EtOH) 292 ($\Delta\epsilon$ 2.3), 300 ($\Delta\epsilon$ 2.5); ^{1}H NMR data see Table 1; ^{13}C NMR data see Table 2; HRESIMS *m*/*z* 381.2795 $[M + H]^+$ (calcd for $C_{26}H_{37}O_2$ 381.2794).

Chromarol C (10): clear oil; $[\alpha]^{27}_D = 10°$ (*c* 0.17, EtOH); CD (EtOH) 280 ($\Delta\epsilon$ 2.2), 300 ($\Delta\epsilon$ 2.6); ^{1}H NMR data see Table 1; ^{13}C

(42) Tasdemir, D.; Concepción, G. P.; Mangalindan, G. C.; Harper, M. K.; Hajdu, E.; Ireland, C. M. *Tetrahedron* **2000**, *56*, 9025−9030.
(43) Maxwell, A.; Rampersad, D. *J. Nat. Prod.* **1989**, *52*, 614−618.
(44) Salva, J.; Faulkner, D. J. *J. Org. Chem.* **1990**, *55*, 1941−1943.

NMR data see Table 2; HRESIMS *m/z* 381.2796 $[M + H]^+$ (calcd for $C_{26}H_{37}O_2$ 381.2794).

Chromarol D (11): clear oil; $[\alpha]^{27}_D = 7°$ (*c* 0.13, EtOH); CD (EtOH) 280 ($\Delta\epsilon$ 2.2), 300 ($\Delta\epsilon$ 2.6); ^{1}H NMR data see Table 1; ^{13}C NMR data see Table 2; HRESIMS *m/z* 381.2796 $[M + H]^+$ (calcd for $C_{26}H_{37}O_2$ 381.2794).

Chromarol E (12): light yellow oil; $[\alpha]^{27}_D = 3°$ (*c* 0.03, EtOH); CD (EtOH) 290 ($\Delta\epsilon$ 2.1), 305 ($\Delta\epsilon$ 2.7); ^{1}H NMR data see Table 1; ^{13}C NMR data see Table 2; HRESIMS *m/z* 409.2742 $[M + H]^+$ (calcd for $C_{27}H_{37}O_3$ 409.2743).

Synthesis of Chromane Derivatives. Chromane derivatives were prepared according to the method of Kalena et al.[34] In general, 1.5 g of the catalytic sulfonic acid cation-exchange resin, Amberlyst 15 (Sigma-Aldrich), was stirred in dry THF (15 mL) under reflux at 65−75 °C. Approximately 500 mg of phenols was added to the resin, followed by 1.1 molar equiv of diene in hexane (5 mL) over 2 h. Following an additional hour of stirring under reflux, the heat source was removed and 25 mL of Et_2O was added. The resin was filtered by vacuum filtration and rinsed with acetone (75 mL). The crude product mixture was purified by HPLC, affording purified chromane.

2,2-Dimethyl-6-hydroxychromane (25). Hydroquinone (**35**) (500 mg) was reacted with isoprene (0.9 mL) as described. The crude product was purified by preparative HPLC (40−80% CH_3CN), yielding **25** (53% yield): white crystalline solid (from hexanes−Et_2O); ^{1}H NMR ($CDCl_3$, 500 MHz) δ 6.65 (1H, d, J = 8.5 Hz, H-8), 6.59 (1H, dd, J = 8.5, 3.0 Hz, H-7), 6.56 (1H, d, J = 3.0 Hz, H-5), 2.71 (2H, t, J = 7.0 Hz, H-4), 1.77 (2H, t, J = 7.0 Hz, H-3), 1.32 (6H, s, C-2 methyls); ^{13}C NMR ($CDCl_3$, 500 MHz) δ 148.7 (s, C-6), 147.9 (s, C-9), 121.9 (s, C-10), 117.9 (d, C-8), 115.6 (d, C-5), 114.6 (d, C-7), 74.1 (s, C-2), 32.9 (t, C-3), 26.8 (q, C-2 methyls), 22.7 (t, C-4); HRESIMS *m/z* 179.1071 $[M + H]^+$ (calcd for $C_{11}H_{15}O_2$ 179.1072).

Acetylation of 25 (29). A 50 mg portion of **25** was dissolved in 1 mL of dry pyridine. The mixture was stirred while 1 mL of acetic anhydride was added. The mixture continued to stir at room temperature for 24 h until it was aspirated and added to 25 mL of DI H_2O that was extracted with 20 mL of EtOAc (×3). The crude product was applied to PTLC (CH_2Cl_2−MeOH, 99:1), yielding **29** as a white crystalline solid (90% yield): ^{1}H NMR ($CDCl_3$, 500 MHz) δ 6.77 (1H, d, J = 2.5 Hz, H-5), 6.73 (1H, dd, J = 9.0, 2.5 Hz, H-7), 6.66 (1H, d, J = 9.0 Hz, H-8), 2.75 (2H, t, J = 6.5 Hz, H-4), 2.20 (3H, s, OCO*CH*$_3$), 1.77 (2H, t, J = 6.5 Hz, H-3), 1.28 (6H, s, C-2 methyls); ^{13}C NMR ($CDCl_3$, 500 MHz) δ 170.6 (s, O*C*OCH$_3$), 151.7 (s, C-9), 143.7 (s, C-6), 121.8 (d, C-5), 121.7 (s, C-10), 120.2 (d, C-7), 117.3 (d, C-8), 74.2 (s, C-2), 32.3 (t, C-3), 25.8 (q, C-2 methyls), 22.2 (t, C-4), 19.7 (q, OCO*C*H$_3$); HRESIMS *m/z* 221.1183 $[M + H]^+$ (calcd for $C_{13}H_{17}O_3$ 221.1178).

2-Methyl-2-(4-methylpent-3-enyl)-6-hydroxychromane (28). Hydroquinone (**35**) (500 mg) was reacted with the diene β-myrcene (1.8 mL) as described. The crude product was purified by preparative and semipreparative HPLC (20−100% CH_3CN), yielding 110 mg of **31** (19% yield): clear oil; ^{1}H NMR (CD_3OD, 500 MHz) δ 6.50−6.46 (3H, m, H-5, H-7, H-8), 5.08 (1H, t, J = 7.5 Hz, H-3′), 2.66 (2H, t, J = 6.5 Hz, H-4), 1.80−1.39 (6H, m, H-4, H-1′, H-2′), 1.63, 1.56, and 1.21 (each 3H, s, −CH_3); ^{13}C NMR (CD_3OD, 500 MHz) δ 150.0 (s, C-6), 147.1 (s, C-9), 131.1 (s, C-4′), 124.3 (d, C-3′), 121.8 (s, C-10), 117.4 (d, C-8), 115.0 (d, C-5), 114.2 (d, C-7), 75.3 (s, C-2), 39.2 (t, C-1′), 31.1 (t, C-3), 24.7 and 23.2 (each q, C-2 methyl and C-5′), 22.1 (t, C-4 and C-2′), 16.4 (q, C-6); HRESIMS *m/z* 247.1701 $[M + H]^+$ (calcd for $C_{16}H_{23}O_2$ 247.1698).

2,2-Dimethyl-7-hydroxychromane (31). Resorcinol (**37**) (300 mg) was reacted with isoprene (0.5 mL) as described. The crude product was purified by repeated preparative HPLC (33−45% CH_3CN), yielding 60 mg of **31** (15% yield): clear oil; ^{1}H NMR ($CDCl_3$, 500 MHz) δ 6.84 (1H, d, J = 8.5 Hz, H-5), 6.27 (1H, dd, J = 8.5, 2.0 Hz, H-6), 6.15 (1H, d, J = 8.5 Hz, H-8), 2.68 (2H, t, J = 7.0 Hz, H-4), 1.76 (2H, t, J = 7.0 Hz, H-3), 1.29 (6H, s, C-2 methyls); ^{13}C NMR ($CDCl_3$, 500 MHz) δ 158.8 and 157.2 (s, C-7 and C-9), 131.0 (d, C-5), 120.6 (s, C-10), 110.1 (d, C-6), 98.4 (d, C-8), 73.9 (s, C-2), 32.7 (t, C-3), 26.5 (q, C-2 methyls), 22.3 (t, C-4); HRESIMS *m/z* 179.1068 $[M + H]^+$ (calcd for $C_{11}H_{15}O_2$ 179.1072).

2,2-Dimethyl-5,7-dihydroxychromane (32). Phloroglucinol (**36**) (600 mg) was reacted with isoprene (1 mL) as described. The crude product was purified by preparative HPLC (15−65% CH_3CN), yielding **32** (45% yield): light yellow oil oil; ^{1}H NMR (acetone-d_6, 500 MHz) δ 5.94 and 5.78 (each 1H, s, H-6 and H-8), 2.53 (2H, t, J = 7.0 Hz, H-4), 1.71 (2H, t, J = 7.0 Hz, H-3), 1.24 (6H, s, C-2 methyls); ^{13}C NMR (acetone-d_6, 500 MHz) δ 156.8, 156.2, and 155.7 (s, C-5, C-7, and C-9), 100.0 and 95.5 (d, C-6 and C-8), 94.6 (s, C-10), 73.6 (s, C-2), 32.5 (t, C-3), 26.3 (q, C-2 methyls), 16.7 (t, C-4); HRESIMS *m/z* 194.0944 $[M + H]^+$ (calcd for $C_{11}H_{14}O_3$ 194.0943).

Lipoxygenase Inhibition Assay. Human reticulocyte 15-lipoxygenase (15-hLO), human platelet 12-lipoxygenase (12-hLO), and soybean 15-lipoxygenase (15-sLO) were expressed and purified as previously described.[5,45] The IC_{50} values for compounds **1**−**27** against all three enzymes were determined as outlined in our prior disclosures.[5,46] Briefly, all inhibitors and enzyme substrates were dissolved in MeOH (1 mg/mL) and added to 2 mL of buffer under constant stirring. After a brief equilibration, 15-hLO (25 mM HEPES, pH 7.5), 12-hLO (25 mM HEPES, pH 8), or 15-sLO (100 mM borate, pH 9.2) was added, and the enzyme activity was monitored on the basis of the rate of diene product formation at 234 nm at room temperature. Multiple data points inclusive of the 50% inhibitory concentration were acquired and the data fit to a simple saturation curve. The IC_{50} value determination of compound **25** in the presence of ascorbate was performed in HEPES pH 7.5 buffer with the addition of 0.5 mM ascorbate. At this concentration, ascorbate had no direct effect on lipoxygenase activity.

Redox Inhibition Studies. Characterization of a redox mode of inhibition of compounds against lipoxygenases was performed using 15-sLO because this enzyme possesses an active-site configuration that is analogous to that found in human 15-lipoxygenases. The 15-sLO contains several tryptophan moieties that are spectroscopically sensitive to the oxidation state of the active-site iron atom, making it an appropriate model for performing redox studies. Briefly, the iron atom in the model lipoxygenase, 15-sLO, was activated to the ferric species with 13-hydroperoxy-9(*Z*),11(*E*)-octadecadienoic acid (HPOD). The oxidation status of the 15-sLO was monitored by fluorescence (excitation, 280 nm; emission, 328 nm) while test compounds were added to the reaction cell containing 2 mL of borate buffer (pH 9.2) at room temperature with constant stirring. A relative increase in the fluorescence signal intensity indicated a reduction of the 15-sLO active-site iron.[46,47]

Ascorbate Recycling of 6-Hydroxychromane. In these experiments (performed in duplicate), the ferrous iron in 0.26 μM 15-sLO was oxidized in the presence of 1 equiv of HPOD. This was immediately followed by the addition of 1 equiv of chromane **26**, resulting in the complete reduction of the ferric iron. The subsequent addition of an additional 1 equiv HPOD resulted in the reactivation of the lipoxygenase iron center.

In a subsequent experiment, the above procedure was repeated except for the addition of 1 equiv of ascorbate to the incubation buffer. The lipoxygenase was activated as before with HPOD, followed by reduction of the active-site iron by **26**. In contrast to the previous observation, the further addition of 1 equiv of HPOD (total of 2 equiv of HPOD in buffer) resulted in a momentary oxidation of the lipoxygenase iron center, followed by its immediate reduction. However, the subsequent addition of yet another equivalent of HPOD (total of 3 equiv of HPOD in buffer) did result in the complete reactivation of the lipoxygenase active-site iron.

(45) Holman, T. R.; Zhou, J.; Solomon, E. I. *J. Am. Chem. Soc.* **1998**, *120*, 12564−12572.
(46) Finazzi-Agro, A.; Avigliano, L.; Veldink, G. A.; Vliegenthart, J. F. G.; Boldingh, J. *Biochim. Biophys. Acta* **1973**, *326*, 462−470.
(47) Kemal, C.; Louis-Flamberg, P.; Krupinski-Olsen, R.; Shorter, A. L. *Biochemistry* **1987**, *26*, 7064−7072.

Acknowledgment. We thank M. C. Diaz for sponge taxonomic identification. Financial support for this work came from NIH-CA47135 (P.C.), NIH/NIGMS-2R25GM51765 (P.C.), NIH-GM56062-06 (T.H.R.), and ACS RPG-00-219-01-CDD (T.H.R.).

Supporting Information Available: NMR spectra of **8**−**12** and underwater photograph of the *Psammocinia* sp. used in this study. This material is available free of charge via the Internet at http://pubs.acs.org.

JA046082Z